Development of Potential Map for Landslides Induced by the Chi-Chi Earthquake Using Instability Index

Meei-Ling Lin[1], and Yu-Huang Shu[1]
[1]*Department of Civil Engineering, National Taiwan University, Taipei, Taiwan*
E-mail: linml@ntu.edu.tw

ABSTRACT: In Taiwan, sloping lands cover more than 70% of the total area, and the geological condition of Taiwan is fairly fragile. The topography, geology, and tectonic setting make it highly prone to landslides induced by earthquake. In this research, data of the landslides triggered by the Chi-Chi Earthquake was analyzed for assessment of the potential and a predictive model was established for landslide occurrence of the area if similar earthquakes occur. Influence factors were selected and the instability index was used for assessing landslide potential. Through verification of an independent set of ground-based investigation data, results of the prediction model appeared to be satisfactory and can be used for mapping of landslide potential induced by similar earthquake in the future.

1. INTRODUCTION

The Chi-Chi earthquake, 1999 with a moment magnitude of 7.6 struck central Taiwan and caused the largest movement of the earth's crust in the recent 100 years. More than 2400 people were killed, and damage to properties was enormous. Among all types of ground failures, a large number of landslides were triggered, which caused severe damages of properties and life loss. The Bureau of Soil and Water Conservation, Council of Agriculture (SWCB, 2000), reported more than 20,000 cases of ground variation, and the reconnaissance report by National Center for Research on Earthquake Engineering (NCREE, 2000) documented 463 ground-based investigations of the landslide cases. The objective of this research is to analyze the landslide data for the landslide potential assessment, and to establish a predictive model for landslides induced by the earthquake. The research area chosen in this study is along the Cherlungpu fault close to the central range mountain area, where a large number of landslides occurred during the Chi-Chi Earthquake. The research area is between 120^o 36' to 121^o 01' east longitude, and 23^o 33' to 24^o 22' north latitude, the Transverse Mercator 2^o coordinates of (209600- 25300) in x- direction, and (2606400- 2693700) in y- direction as shown in Figure 1. Administrative districts in the research area include parts of Taichung City, Nantou County, Miaoli County, Changhua County, Yunlin County, and Chiayie County.

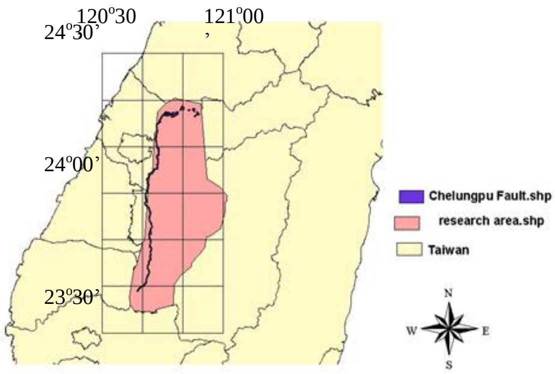

Figure 1 Location of research area and Cherlungpu Fault

2. DATABASE OF LANDSLIDES TRIGGERED BY CHI-CHI EARTHQUAKE

The Chi-Chi Earthquake triggered a large number of landslides in central Taiwan. Liao (2000) identified locations and areas of landslides and suggested that the number of landslides with areas larger than 625 m^2 is 9272, and the aggregated landslide area is 127.8 km^2. Most of the landslides induced by the Chi-Chi Earthquake were located in central Taiwan to the east of the fault according to the reconnaissance reports by NCREE (2000) and Bureau of Soil and Water Conservation (SWCB, 2000). In order to perform the analysis, the results of ground variation investigation by the Bureau of Soil and Water Conservation (2000) were used together with other basic data such as geological conditions, digital terrain models, ground motion records, etc. for analysis and construction of the model. The databases for the geo-morphological and hydrological properties of the study area were established. The landslide data of the NCREE (2000) report were then applied for verifications of the assessment model.

2.1 Landslide investigation and database

The landslide investigation supported by Bureau of Soil and Water Conservation, Council of Agricultural (2000) was based on pixel variation of the Spot satellite images taken before and after the earthquake, and some verification was made by comparing ground variation results to aerial photographs taken after the earthquake. A total of 21969 cases of ground surface variation were identified through the investigation. Some field inspections were also conducted to verify the identified ground variation results. For each identified ground surface variation, the location, elevation, slope aspect, slope angle, and landslide area are documented. The landslide data used in this study were screened due to limitation on resolution of the digital terrain model (DTM) before the earthquake, and to ensure the reasonability of data. The rules for data screening are as follows.

1. Landslide area: The digital terrain model (DTM) available before the earthquake has a resolution of 40m × 40m, the landslides with areas smaller than 1600m^2 could not be properly represented and analyzed. In addition, 68 landslides with areas larger than 100,000 m^2, including Tsao-Ling Landslide and Jer-Fen-Err Mountain Landslide, were not considered to avoid the possible effects of overweighting.
2. Variations of elevation: The identified data points were based on the pixel variations of the satellite images before and after the earthquake. With the landslide occurrence, the ground elevation near the slope crest will be lowered after the landslide, and the ground elevation near the slope toe will be raised due to the mass movement downslope. Therefore, variation of elevations after the earthquake for each landslide data set was checked, and the data sets with unreasonable variation in elevations were omitted.

After the screening process, the number of data sets in this study reduced to 2658, and their distribution is as shown in Figure 2. In addition, the database of ground-based investigations of 436 landslides by NCREE (2000) was used for model verification. Data

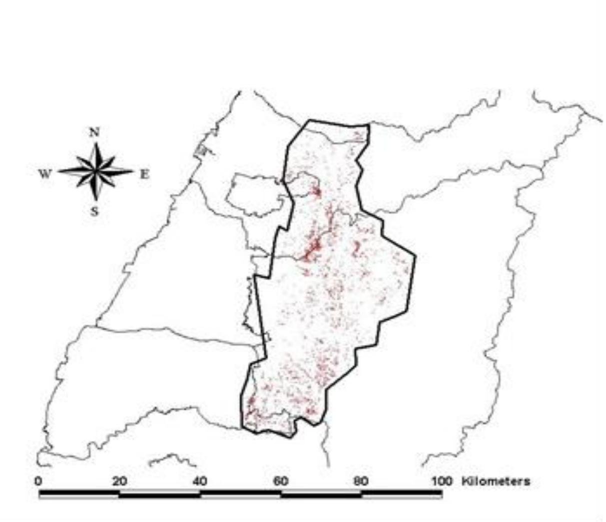

Figure 2 Distribution of screened ground variation data from SWCB (2000)

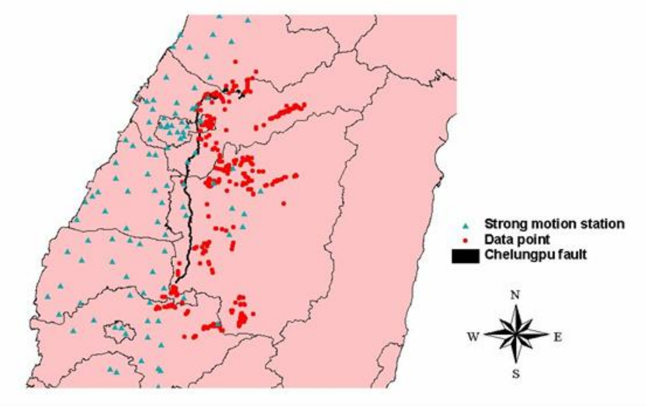

Figure 3 The locations of 436 cases documented in NCREE (2000) and distribution of strong motion stations.

items documented in field investigation included location, type of slope failure, slope aspect, slope angle, and area of landslide, distribution of the landslide data was as shown in Figure 3.

2.2 Other baseline database

To perform the potential analysis, it was necessary to obtain the topographic data before the landslides. The ground topography changed after the landslide, thus the information obtained from the field investigation cannot be used for potential analysis. Therefore, the topographical factors used in the potential analysis were generated based on the digital terrain model established before the earthquake. The basic information required for generating the pre-landslide database is as follows,

1. Digital terrain model：In this research, the digital terrain model based on aerial photos with a scale of 1/5000 was used, and the resolution was 40m × 40m.
2. Geological formation：The geological map produced by the Central Geological Survey (1990) with a scale of 1/250,000 was used as shown in Figure 4.
3. Locations of the Cherlungpu Fault and epicenter of the Chi-Chi Earthquake: The locations of the Cherlungpu Fault and the epicenter of the Chi-Chi Earthquake (120.75^{o} east longitude, 23.87^{o} north latitude) are as shown in Figure 5, from which the distance factors to the fault and epicenter could be determined.
4. Road map: The road map produced by the Ministry of Interior was used, and the scale was 1/25000.
5. Stream map: The stream map produced by the Ministry of Economic Affair with the scale of 1/25000 in 1999 was used.

For the ground motion considered in this research, records of the 324 strong motion stations of the Central Weather Bureau were used, and the locations of these stations were shown in Figure 3. The parameters used to characterize ground motion included the Arias intensity (Arias,1970) of horizontal ground motion and the vertical ground acceleration as discussed in the follow,

1. Arias intensity of horizontal ground motion: For the horizontal ground motion, the Arias intensity of ground acceleration was used, which possessed the energy signature of earthquake and was not affected by the direction of ground motion. The Arias intensity, I_a, is determined as,

$$I_a = \frac{\pi}{2g}\int_0^{Td}[a(t)]^2\,dt \tag{1}$$

where, a(t)：time history of horizontal ground acceleration (m/sec^2)
T_d：time duration (sec)
g : acceleration of gravity (m/sec^2)

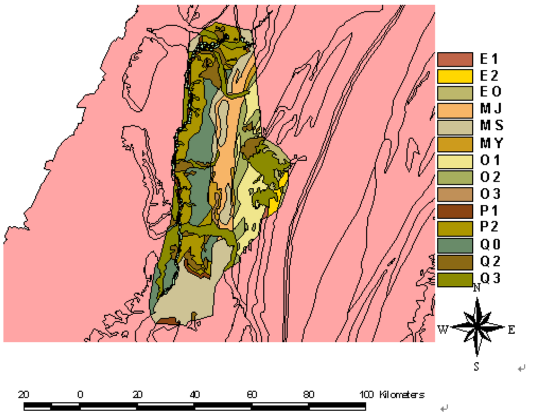

Symbol	Formation Name
E	Pilushan Formation
E1	Shihpachungchi Formation
E2	Tachien Sandstone
EO	Hsitsun Formation,Chiayang Formation
MJ	Juifang Group & its equivalents
MS	Sanhsia Group & its equivalents
MY	Yehliu Group & its equivalents
O1	Szeleng Sandstone,Meichi Sandstone,Paileng Formation
O2	Tatungshan Formation,Kankou Formation,Shuichangliu Formation
O3	Wuchihshan Formationand,Wentzekeng Formation,Tsukeng Formation
P1	Chinshui Shale its equivalents
P2	Cholan Formation and its equivalents
Q0	Toukoshan Formation,Pinanshan Conglomerate,
Q2	Terrace Deposits
Q3	Alluvium

Figure 4 The 1/250,000 geological map of the research area

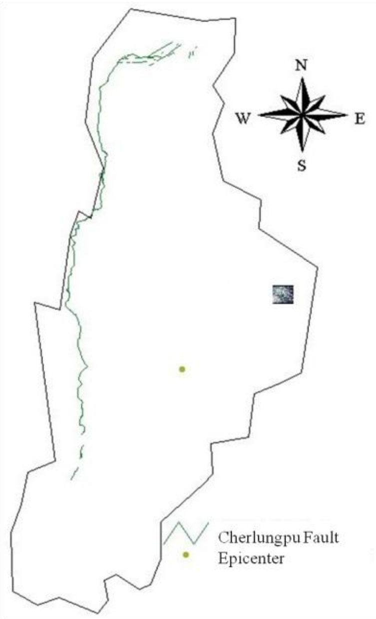

Figure 5 The locations of the Cherlungpu Fault and the epicenter of the Chi-Chi Earthquake, and location of the aerial photo used for development of grid-based procedures for regional potential map

The time records in the N-S and E-W directions were combined and time duration used in the integration lasted through the whole recorded duration, which was approximately 90 seconds.

2. Peak vertical ground acceleration: the peak vertical ground acceleration was considered as a separate parameter.

3. INFLUENCE FACTORS

In order to perform the potential analysis, possible influence factors needed to be determined. The major parameters affecting the regional landslide potential caused by earthquakes include the geo-morphological properties of the terrain, the geological formations, and the causal factors which were the characteristics of the ground motion induced by the earthquakes. Various influence factors were used by different researchers (Keefer, 1984, 2000, Hung, et.al. 2000, Lin and Tung, 2004), and it was found that the factors influencing the landslides included topographic characteristics of the slope, geological formations, land development, and ground motion characteristics. Based on previous researches, ten factors were selected to take into account the effects of topography, geology, land development, and ground motion. The ten influence factors chosen are: elevation, slope angle, slope aspect, geological formation, distance to fault, distance to epicenter, distance to road, distance to river, Arias intensity of the horizontal ground motion, and the vertical peak ground acceleration. The distance to road was used to provide the possible effects of disturbance to the slope due to construction of road. The distance to river would provide the indication of erosion to the toe of slope which might affect the stability of slope. For the area close to the epicenter as the study area in this research, the vertical ground motion could have a significant effect on the landslide, and thus was taken into account. In addition to the ground motion, for the landslide triggered by earthquake, the faulting action and ground rupture had a significant effect on the landslide (Keefer, 1984, 2000, Tibaldi, et al. 1995), and therefore, the distance to the fault was also included as an influence factor. The spatial distributions of the ten factors were extracted and derived from the baseline and documented landslide data of the study area. In order to establish a regional landslide potential map, the extraction of the influence factors is determined for each pixel based on the resolution of the DTM. Derivations of the factors were performed using spatial analysis in the Geographic Information System (GIS) as described in the follow.

1. Elevation: The elevation was determined for each pixel of the DTM.
2. Slope angle: The slope angle was determined for each pixel based on the neighboring topography using DTM.
3. Slope aspect: The slope aspect was defined by the unit vector in the outward direction of slope of each pixel, and represented in degree clockwise from the north.
4. Geological formation: The geological formation was obtained by overlaying the geological map with DTM, and the property was assigned to each grid accordingly. The resulting distribution was descriptive and the factor was categorical.
5. Distance to fault: The distance to fault was determined as the shortest surface distance to the Cherlungpu Fault according to Campbell and Bozorgnia (1994).
6. Distance to epicenter: The distance to epicenter was determined as the surface distance to the epicenter.
7. Distance to road: The distance to road was determined as the shortest surface distance to the road based on the road map.
8. Distance to river: The distance to river was determined as the shortest surface distance to river channel based on the river map.
9. Arias intensity of the horizontal ground motion: The Arias intensity of the horizontal ground motion was calculated based on Eq. 1 for records of each strong motion station inside and nearby the study area. The contour of the Arias intensity was established accordingly, and the Arias intensity at each pixel was then interpolated from the contour distribution using inverse distance weighting method.
10. Vertical peak ground acceleration: To consider the effects of vertical ground motion, the contour of peak vertical acceleration was constructed using the strong motion station records, and the peak vertical acceleration of each pixel was interpolated from the contour distribution using inverse distance weighting method.

Among the ten influence factors, some factors had only qualitative descriptions and were termed as categorical variables, such as the geological formations of the landslides. However, other factors were quantified variables with numerical values. In order to combine the two types of variable in the same model, one type of the variable should be transferred into the other type. In this research, the instability index was used for establishment of the potential analysis model, and in which the categorical variables were used. Thus, the

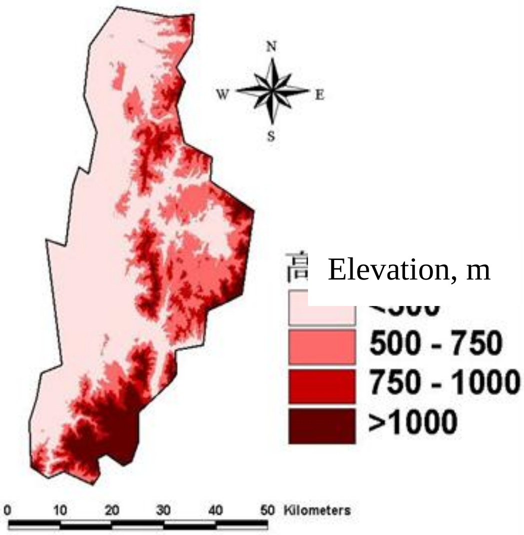

Figure 6 Distribution of elevation factor treated as a categorical parameter

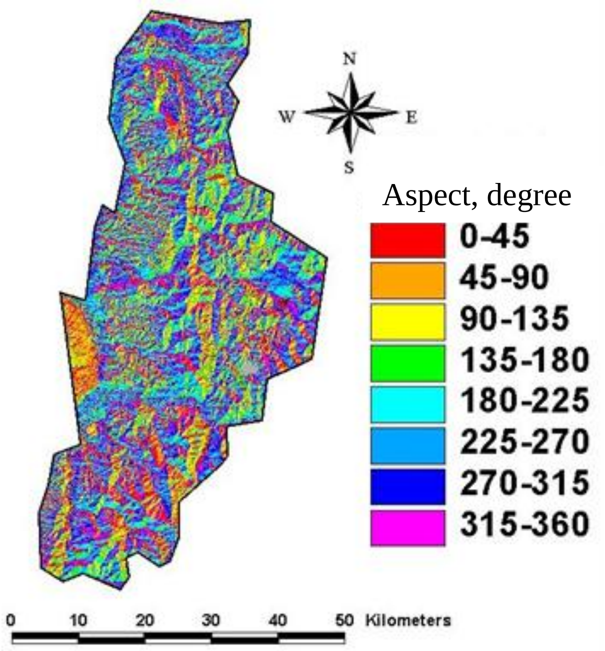

Figure 7 Distribution of aspect as degree clockwise from north direction and treated as a categorical parameter

continuous quantified variables were transferred to categorical variables. Therefore the factor with quantitative values was broken into groups of various value ranges, and the factor became categorical. For the factor with values within specified range, the distribution of the values was examined. Variable with distinct different groups of distribution was broken into groups using natural break, and equal interval was assigned within each subgroup. For the quantitative factors with continuous values and no distinctive distribution, equal interval was assigned to break the continuous values into groups with different ranges. Examples of the quantitative factors thus treated are as shown in Figure 6 and Figure 7 for elevation factor and slope aspect factor where equal interval was assigned. The distribution of slope angle factor is as illustrated in Figure 8 with the specific range of values and equal interval.

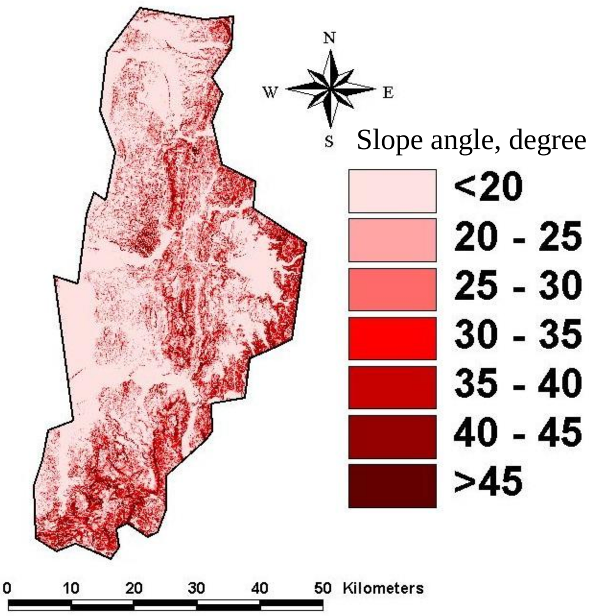

Figure 8 Distribution of slope angle factor with distinctive range and treated as a categorical parameter

4. INSTABILITY INDEX AND FACTOR SIGNIFICANCE

In this study, instability index method used by Chien (1992) was modified for construction of assessment model for the landslide potential. The landslide ratio was used as the parameter for rating of each influence factor. The landslide ratio, S_i, is defined as the ratio of landslide area to the total area for a specific subgroup within a given influence factor, and is expressed as:

$$S_i = \frac{A_{landslide,i}}{A_{total,i}} \tag{2}$$

where $A_{landslide,i}$ is the landslide area and $A_{total,\,i}$ is the total area for the ith subgroup of the given factor. For a given influence factor, the landslide ratio, S_i , for each subgroup within the factor was determined, and then normalized to a value ranging from 1 to 10, which was termed as instability index. The instability index, D_i, for potential rating of the *i*th subgroup in a given factor can be calculated as:

$$D_i = \frac{9(S_i - S_{\min})}{(S_{\max} - S_{\min})} + 1 \tag{3}$$

in which S_{max} and S_{min} are the maximum and minimum values of landslide ratio among all the subgroups of a given factor. The overall instability index *D* of a designated event is the combination of all the instability index, D_j , of each potential influence factor with $j = 1,2,\ldots,10$, and is as shown in the following equation:

$$D = \prod_{j=1}^{10} D_j^{W_j} \tag{4}$$

where W_j is the weighting of each influential factor. With instability index of each potential factor ranging from 1 to 10 and weighting, W_j summing up to 1, the value of the overall instability index is in the range from 1 to 10, with value close to 10 indicating a very high potential, and a value close to 1 indicating low potential. The weighting of each potential influence factor provides an indication of the significance of each factor, weighting with higher values indicating more significant and value close to zero indicates little effect of the factor on the overall instability index, and thus the factor is insignificant. The computation of the weighting of each factor is based on the variance of the distribution of landslide ratio within each factor. The variance of each influence factor, V_j, could be determined as,

$$V_j = \frac{\sigma_j}{X_j} \times 100(\%) \tag{5}$$

in which,

V_j : the variance of all subgroups rated in the *j*th factor,

σ_j : the standard deviation of all subgroups rated in the *j*th factor,

X_j : the mean value of all subgroups rated in the *j*th factor.

The weighting of each factor, W_j, is then computed as the ratio of *j*th variance over the summation of variances of all factors as,

$$W_j = \frac{V_j}{\sum_{j=1}^{10} V_j} \tag{6}$$

The value of each weighting, W_j, is in the range from 0 to 1, and the summation over all the weightings equals 1.

For the instability index used for evaluation of the landslide potential, the influence factors should be categorical variables. All the quantitative factors were transferred into categorical variables as discussed in the previous section. Effects of different breaking of subgroups within each influence factor were rated based on the outcome landslide ratio using variance analysis, and testing of the significance of each influence factor was conducted. It was found that all of the ten influence factors with the breakings assigned within each factor appeared to be within the significant level, with the degree of significance rated from high to low as: slope angle, geological formation, distance to fault, distance to road, Arias intensity of the horizontal ground motion, elevation, vertical peak ground acceleration, distance to river, distance to epicenter, and slope aspect. The factorial analysis of the co-variances (ANOCOVA) was performed on the instability index to examine the correlation and interaction among influence factors. To perform factorial ANACOVA for interaction of two factors, the variance of one factor was analyzed while the other factor changed from one subgroup to other subgroups. Results of the factorial ANOCOVA indicated that the correlations among the factors were not significant, and the effects of each influence factor on the landslide potential were significant and fairly independent.

5. INSTABILITY INDEX AND LANDSLIDE POTENTIAL

With all the rating of the influence factor and the weightings of factors determined, the final instability index can be computed as:

$$D = D_{elevation}^{\;0.07} \times D_{aspect}^{\;0.05} \times D_{slope}^{\;0.21} \times D_{d-fault}^{\;0.13} \times D_{d-epi}^{\;0.06}$$

$$\times D_{d-road}^{\;0.1} \times D_{d-river}^{\;0.06} \times D_{geo}^{\;0.19} \times D_{PGA-V}^{\;0.06} \times D_{Ia}^{\;0.07} \qquad (7)$$

where, $D_{elevation}$, D_{aspect}, D_{slope}, $D_{d\text{-}fault}$, $D_{d\text{-}epi}$, $D_{d\text{-}road}$, $D_{d\text{-}river}$, D_{geo}, $D_{PGA\text{-}V}$, and D_{Ia} are the instability indices of the ten influence factors, respectively. The distribution of the rated instability indices of all the 2658 landslides is as shown in Figure 9. In Figure 9, the values of the instability index distributed from about 1.4 to 9.1 with a mean value of 4.53 and about 79% of the landslide cases had values ranging from 3 to 6. Observing Figure 9, most of the landslides were with instability index of higher than 3, and thus the slopes with instability index smaller than 3 were considered as with low potential. For slopes with instability index larger than 4.5 which was about the mean value of all slopes were considered as high potential. The distribution of landslide potential for all 2658 landslides is as shown in Figure 10. In Figure 10, the areas right next to the Cherlungpu Fault have intermediate to low potential, while areas further to the east of the Cherlungpu Fault and close to the Swungtung Fault have high potential, and then intermediate potential further to the east. This may due to the natural terrain for the areas near the Cherlungpu Fault have mild slope, and the terrains further to the east are usually steeper as shown in the slope angle distribution in Figure 8.

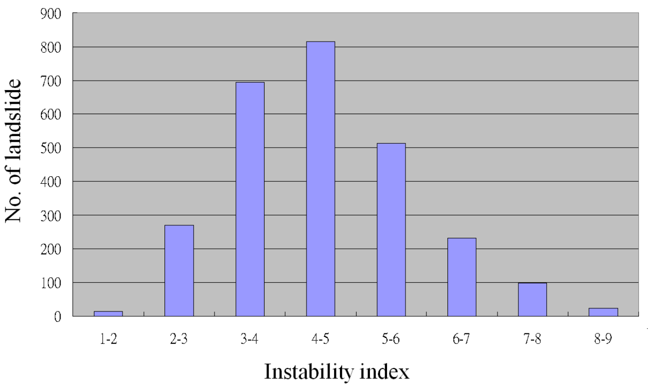

Figure 9 Distribution of the rated instability indices of the 2658 landslides

The weighting of each influence factor was calculated based on the variances of distribution as shown in Eq. (6). The resulting coefficients of variances and weightings of the ten influence factors are listed in Table 1. The weighting ranged from 0.05 to 0.21, with the highest weighting for slope angle and lowest weighting for the slope aspect. All of the weightings suggested that the influence factors used were within the significance level. Among the ten influence factors, the slope angle and geological formation have the highest weightings and appear to be the two most significant factors related to earthquake-induced landslide. In general, the landslide

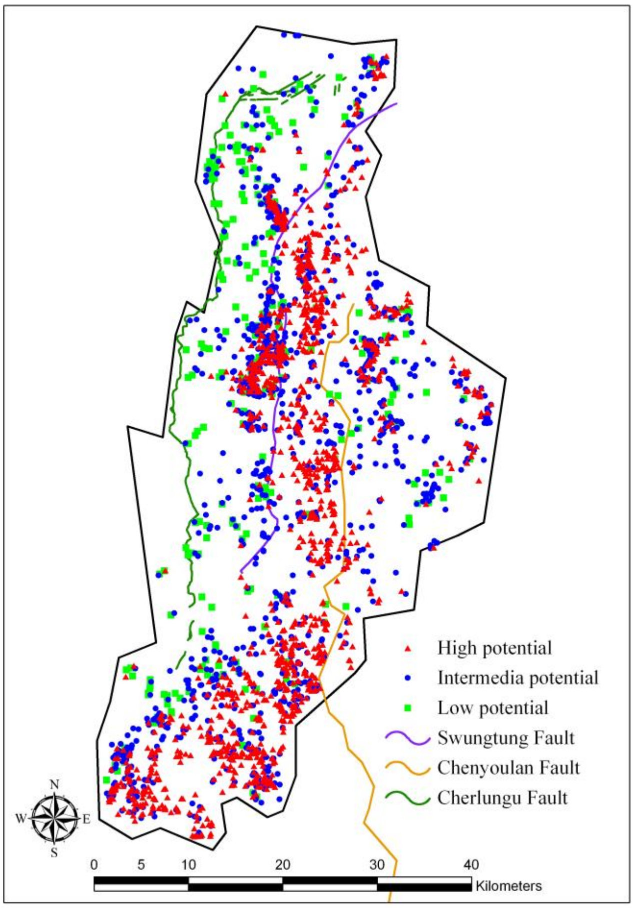

Figure 10 Distribution of the rated landslide potential for 2658 landslides

Table 1 Variance and weighting of the influence factor

Influence factor	Coefficient of variance	Weighting
Elevation	35.06	0.07
Slope aspect	25.07	0.05
Slope angle	98.08	0.21
Distance to fault	60.49	0.13
Distance to epicenter	29.86	0.06
Distance to road	49.54	0.10
Distance to river	28.63	0.06
Geological formation	91.22	0.19
Aria Intensity of horizontal acceleration	27.57	0.06
Peak ground acceleration-vertical	32.87	0.07

potential increases with steeper slope, longer distance to road, higher Arias intensity of the horizontal ground motion, higher elevation, and higher vertical peak ground acceleration. The tendency of the effects of each influence factor was affected by the distribution of the factor itself and terrain. As for the aspect of the slope, the slopes with an aspect in perpendicular to the alignment of fault appeared to have higher landslide potential. Although the weightings of Arias intensity of the horizontal ground motion and vertical peak ground acceleration did not appear to be very high compared to that of other factor, it might be due to the research area selected was a relatively small zone parallel to the fault, and the variations in distributions of the Arias intensity and peak ground acceleration were not much different. The weightings of the vertical peak ground acceleration and Arial Intensity of horizontal ground acceleration were about the same as shown in Table 1, and the analysis of covariance indicated that the interactions of the two factors with other factors were similar. Such results suggested that the effects of earthquake are significant for both horizontal and vertical ground motions, and it might be slightly more significant for the vertical motion because the study area is quite close to the fault and epicenter, and the vertical motion has more significant effects on slope stability.

6. VALIDATIONS AND LANDSLIDE POTENTIAL ASSESSMENT

In order to verify the resulting prediction model, the field investigation data by NCREE (2000) were used. Due to lacking the landslide area data, the locations of the documented cases were super-imposed on the distribution of instability index of each influence factor generated in the analysis model, and the resulting instability index for the 436 cases were computed. The distribution of the values of the instability index was as shown in Figure 11. Comparing the instability index of the ground-based data to that of the data by SWCB (2000) in Figure 9, most ground based-data yielded an instability index higher than 3, and the mean value of the instability index is 4.9, which was larger than the mean value determined from the SWCB data set. Only a distinctive amount of the cases had an instability index smaller than 3, and the computed values appeared to be higher than those of SWCB data, which indicated a higher potential and was reasonable as for the ground-based data. The distribution of landslide potential of the ground based data was as shown in Figure 11, in which the cases with instability index smaller than 3 were designated as with low potential, and cases with instability index larger than 4.5 were assigned as with high potential. The distribution of the landslide potential in Figure 12 appeared to be in a similar trend as Figure 10. Most of the ground based data displayed a landslide potential ranging from intermediate to high, which was reasonable as the ground based data were from field investigations of landslide occurrences. The breakings used for low, intermediate, and high potential were 3 and 4.5, which appeared to be appropriate considering the results of the ground based cases. Although for the ground variation data in Figure 9, there appeared to be more than 200 cases with instability indices smaller than 3, cross-examination suggested that such cases usually were with mild slope and low elevation close to the river valley when comparing their distribution in Figure 10 to Figure 8 and Figure 6. Observing the distribution of the different rating of landslide potential in Figure 12, the low potential cases located close to the Cherlungpu Fault, which might due to the mild terrain in the local area as discussed previously. Most of the high potential cases located in the area about 20km to the east of the Cherlungpu Fault and close to the Swungtung Fault. Such results had a similar trend compared to the distribution of landslide potential by Lin and Tung (2004).

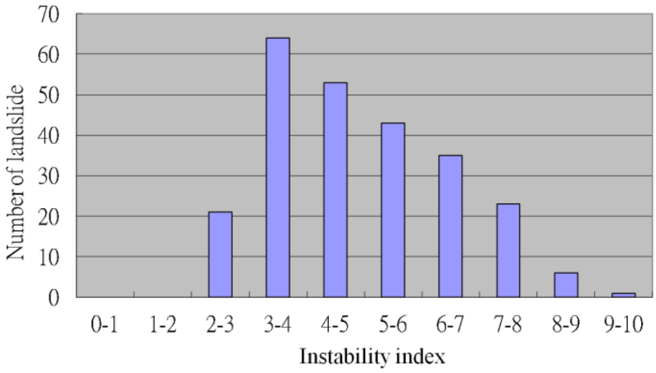

Figure 11 Distribution of the instability index of ground-based data by NCREE (2000)

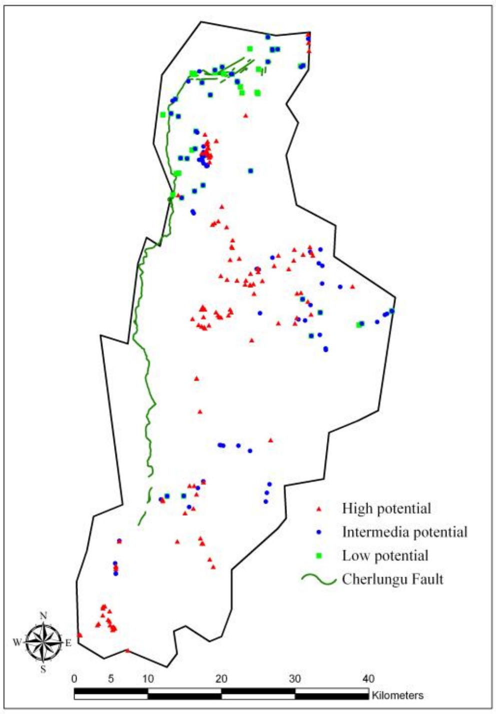

Figure 12 The resulting landslide potential of the ground-based data by NCREE (2000)

When developing the instability index model, 68 landslides with areas larger than 100,000 m^2, including Tsao-Ling Landslide and Jer-Fen-Err Mountain Landslide, were not considered to avoid the possible effects of overweighting. The 68 cases were evaluated using the instability index model to assess the feasibility of the model for large scale landslide. The locations of the 68 cases were super-imposed on the distribution of instability index of each influence factor generated in the model, and the distribution of the instability index for the 68 cases was as shown in Figure 13. For the 68 cases of large area landslide, only 3 cases had instability indices smaller than 3, and the mean value of the instability index was 4.79, which was larger than the mean values from model based on the smaller area landslide. Thus the instability model constructed appeared to yield higher instability index and would be feasible for assessing the potential of large area landslide.

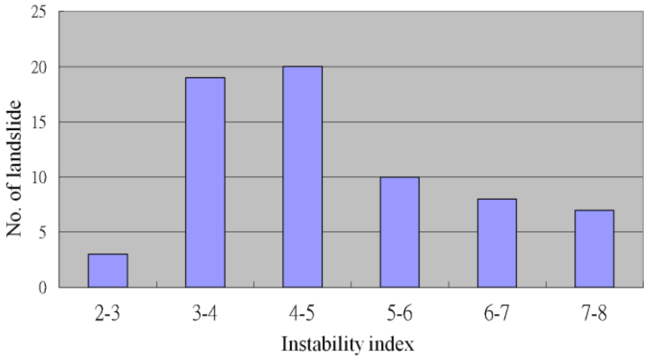

Figure 13 Distribution of the instability index of 68 large area cases

In order to establish a landslide potential map and to perform regional assessment, a grid-based procedure was developed based on the instability index model, and results were verified using aerial photograph. The aerial photo of a small area (Aerial photo ID: R77213) within the study area was selected, and its location was as shown in Figure 5. Landslides triggered by the Chi-Chi Earthquake within the area were identified and mapped as shown in Figure 14. To determine distribution of the landslide potential of the area, a grid of 20m × 20m was superimposed on the aerial map. The gridded map was then superimposed on the distribution of instability index of each influence factor derived in the model, and the instability index was computed grid by grid. Results of the landslide potential predicted using the model was as shown in Figure 15. It was found that only low to intermediate landslide potential grids were obtained from the model, and no high landslide potential was predicted. Comparing the prediction results in Figure 15 to the mapped landslides in Figure 14, the distribution of intermediate potential grids appeared to be quite consistent with the locations of mapped landslides. The number of grids identified as landslide from the aerial photo was 65, and among them 48 grids fell in intermediate potential and 17 grids fell in low potential as predicted by the model. Thus, about 74 % of the identified landslide fell in the intermediate potential zone, and the prediction model appeared to be able to predict the landslide potential reasonably well. However, more grids were predicted as with intermediate potential compared to the identified landslides, and the prediction potential map tended to be conservative. This might due to the area used for prediction was partly in the Pu-Li Basin and partly in the mountain terrain. Therefore, the slope angles of the area varied from mild to steep rapidly within a short distance. To improve the prediction model, the ground variation data might need to be more closely examined to eliminate possible errors in the data, and incorporation of more effective influence factors could be helpful.

Figure 14 Aerial photo (ID: R77213) of a small area with landslides identified and mapped as shaded pixels

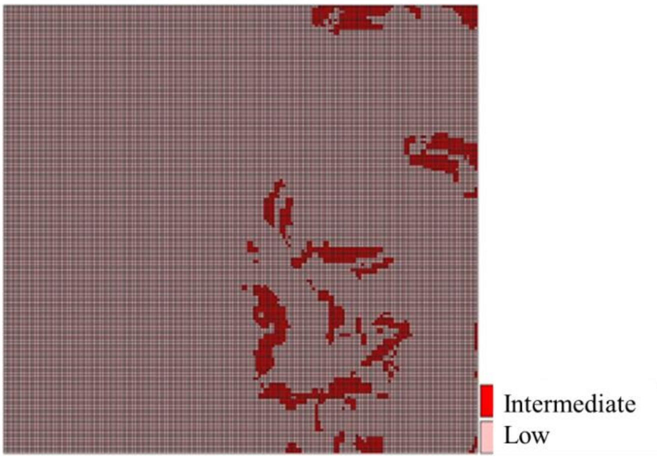

Figure 15 The landslide potential of the area in aerial photo (ID: R77213) predicted by the instability index model

7. CONCLUSION

In this research, a potential analysis was performed on the landslide database established by SWCB (2000) of the landslides triggered by the Chi-Chi Earthquake. Ten influence factors were used for the model, which were elevation, slope angle, slope aspect, geological formation, distance to fault, distance to epicenter, distance to road, distance to river, Arias intensity of the horizontal ground motion, and vertical peak ground acceleration. All influence factors appeared to be significant and relatively independent of each other. A potential analysis was performed and prediction model was established based on the influence factors and instability index was used for potential assessment. The results of prediction using other set of independent ground-based investigation data by NCREE (2000) indicated a consistent trend and with higher instability index. The grid-based procedure was developed based on the assessment model for landslide potential, and prediction of landslide triggered by similar earthquake in the sub-set area appeared to provide satisfactory results, and the resulting potential map can be used as a reference for further hazard mitigation measures. Further improvement of the predictive model requires close examination of the database, and more effctive influence factors can be incorporated.

8. REFERENCES

Arias, A., (1970) A Measure of Earthquake Intensity, in R.J. Hansen, ed. Seismic Design for Nuclear Power Plants, MIT Press, Cambridge, Massachusetts, pp 438-483.

Campbell, K. W., and Bozorgnia, Y., (1994) Near-Source Attenuation of Peak Horizontal Acceleration from Worldwide Accelerograms Recorded from 1957 to 1993, Proceedings, Fifth U.S. National Conference on Earthquake Engineering, Earthquake Engineering Research Institute, Berkeley, California, 1, pp283-292.

Central Geological Survey, (1990) the 1/250,000 geological map of Taiwan

Chien, Lee-Bing, (1995) Quantitative assessment of slope stability using GIS, Master Thesis, Department of Civil Engineering, National Chung-Hsin University, Taichung, Taiwan

Hung, Ju-Jiang. ,Lin, Meei-Ling, Chen, Tien-Chien, and Wang, Kuo-Lung, (2000) "Disasters, Characteristics, and Case Analysis of Slope Failures Caused by Chi-Chi Earthquake", Sino-Geotechnics, 81, pp17-32.

Keefer, D.K., (1984) "Landslides Caused by Earthquakes", Geol. Soc. Am. Bull., 95, pp406-421.

Keefer, D.K., (2000) “Statistical Analysis of an Earthquake-Induced Landslide Distribution – the 1989 Loma Prieta, California Event”, Engineering Geology, 58, pp231-249.

Liao, S. W., (2000) "Landslides Triggered by Chi-Chi Earthquake", thesis for Master degree, Department of Earth Sciences and Insititute of Geophysics, National Central University.

Lin, Meei-Ling, and Chi-Che Tung, (2004) "A GIS-based potential analysis of the landslidesinduced by the Chi-Chi earthquake", Engineering Geology, 71, pp63-77.

National Center for Research on Earthquake Engineering. (2000) Investigation Report of the Geotechnical Hazard Caused by Chi-Chi Earthquake, Taiwan.

The Bureau of Soil and Water Conservation., Council of Agriculture (SWCB). (2000) Investigation of 921 Earthquake(2)- Landslide Investigation and Conservation Strategies.

Tibaldi, A., Ferrari, L. and Pasquare, G. (1995) Landslides Triggered by Earthquakes and Their Relations with Faults and Mountain Slope Geometry – An Example from Ecuador, Geomorphology, 11(3), pp215-226.